CFD Modeling

3

CFD Modeling of Fundamental Phenomena Relevant to Solvent Extraction: An Overview

K. K. Singh*[1,2], R. K. Chaurasiya[1,2], S. Sarkar[1,2], N. Sen[1,2]and S. Mukhopadhyay[1,2]

[1]*Chemical Engineering Division, Bhabha Atomic Research Centre (BARC), Trombay – 400085, INDIA*
[2]*Homi Bhabha National Institute, Anushaktinagar, Mumbai, – 400094, INDIA*

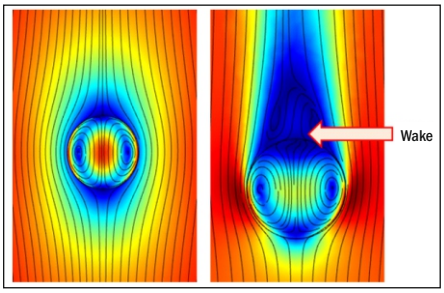

Streamlines inside and outside the drop at Re_p = 0.289 (left) and, Re_p = 254 (right)

ABSTRACT

Solvent extraction is the most important separation process in the nuclear fuel cycle. Different types of solvent extraction equipment are used in different processes used for separation and purification of nuclear materials. Detailed insights into liquid-liquid two-phase flow and mass transfer phenomena are needed for efficient design of solvent extraction equipment to achieve process intensification. CFD modeling of solvent extraction is increasingly being used to have such detailed insights. In equipment-level CFD modeling, the governing equations that need to be solved require appropriate closure equations. These closure equations, such as the equations to estimate drag coefficient or mass transfer coefficient, are usually empirical in nature. Thus, accuracy of equipment-level CFD models depends on the accuracy of the closure equations. To reduce the empiricism in equipment-level CFD models, the closure equations can be obtained in a more fundamental manner by carrying out droplet-level CFD modeling of underlying phenomena. This article provides an overview of CFD modeling of different phenomena relevant to solvent extraction targeted at generation of CFD-based closure equations. The article also provides an overview of CFD modeling of fundamental phenomena relevant to microfluidic solvent extraction which is being explored for intensification of solvent extraction processes.

KEYWORDS: *Breakage, CFD, Coalescence, Drag, Drop, Microfluidics, Slug, Solvent Extraction*

Introduction

Solvent extraction plays a very important role in the nuclear fuel cycle starting from production of nuclear pure uranium from its ore to spent nuclear fuel reprocessing. The processes for production of other nuclear materials such as zirconium, thorium etc. also involve solvent extraction as the key processing step [1,2]. Depending upon specific process requirements, different solvent extraction equipment such as mixer-settler, air pulsed column, rotating disc contactor, annular centrifugal extractor are used for carrying out solvent extraction. These equipment basically differ in the mode of providing energy to generate liquid-liquid dispersion to ensure fast mass transfer. However, the similarity in their functioning is that all involve liquid-liquid two-phase turbulent flow, breakage and coalescence of droplets, and interphase mass transfer. Owing to the complexity of the phenomena prevalent inside solvent extraction equipment, the approach to design solvent extraction equipment has been based on experimentation at bench-scale, pilot-scale setups and using empirical correlations reported in literature over the years [3]. This design approach leads to equipment having high design margins. With more and more thrust being giving on process intensification, it is necessary to design efficient contactors with bare minimum design margins. However, this makes a thorough and fundamental understanding of the functioning of the equipment a prerequisite.

*Author for Correspondence: K.K. Singh
E-mail: kksingh@barc.gov.on

Computational Fluid Dynamics (CFD) modeling is the most useful tool to understand the flow physics in solvent extraction equipment [4]. There are different levels of CFD models of solvent extraction equipment. The simplest is the one in which drop diameter is assumed to be known and uniform and CFD simulations are targeted to obtain the flow field of the continuous phase and dispersed phase and spatial distribution and average volume fraction (hold-up) of the dispersed phase. These simulations typically involve solving continuity equations and momentum equations of the two phases along with an appropriate model of turbulence. The two phases exert drag force on each other and, thus, there is a term representing interphase momentum exchange in the momentum equations of both phases. To model this term, an appropriate model for drag force is needed. The drag models typically used in CFD models are the drag models reported in literature. Most of these drag models are empirical models based on experiments conducted in simple settings such as a single solid particle settling in a quiescent liquid. The reported drag models usually do not incorporate the physics such as the effect of turbulence on drag force and effect of internal circulations inside the drop on drag force–a phenomenon which is unique to liquid-liquid flows and is not applicable for gas-liquid or solid-liquid flows. In many cases, the results obtained by using these drag models do not match with the experimental observations. This necessitates modification in drag models to ensure better match with experimental data [5]. To get rid of the two-phase CFD models from such empiricism, it is necessary to thoroughly understand the drag phenomenon

for liquid-liquid systems. With highly controlled droplet-level experiments practically ruled out, CFD modeling becomes a very important tool to understand this phenomenon. This is one of the fundamental aspects of liquid-liquid two-phase flow which needs to be understood by carrying out CFD simulations at droplet-level.

The next higher level of CFD modeling of solvent extraction equipment is CFD-PB (Computational Fluid Dynamics–Population Balance) modeling in which the assumption of constant and uniform drop diameter is done away with [6]. The drop diameter is estimated by solving population balance equations along with flow equations. The population balance equations consider convective and dispersive transport of drops, breakage and coalescence of drops. The terms corresponding to breakage and coalescence of drops appear as source or sink terms in the population balance equations. The mathematical description of these terms requires breakage and coalescence kernels. The breakage and coalescence kernels reported in literature are empirical or semi-empirical in nature. Thus, the results of CFD-PB simulations depend on selection of the breakage, coalescence kernels and the constants therein [7]. To rid of the CFD-PB models from empiricism, the empirical or semi-empirical breakage, coalescence kernels should be replaced with fundamentally obtained breakage and coalescence kernels for which CFD simulations dedicated to study breakage and coalescence phenomena under different types of flow fields are required. Thus, study of breakage and coalescence is yet another fundamental aspect that must be studied separately to reduce empiricism in equipment-level CFD-PB models.

The ultimate objective of CFD modeling of solvent extraction equipment is to predict their mass transfer performance. To predict mass transfer, a CFD model which solves species transport equations in both phases along with flow and population balance equations should be used. Such a model is computationally very expensive and in literature only very few such studies have been reported [8]. The other way to predict mass transfer performance is by using axial dispersion model in which the inputs of hydrodynamics variables may come from empirical correlations or from the results of CFD simulations [9,10]. In either approach of mass transfer modeling, an appropriate model to estimate mass transfer coefficient for interphase mass transfer is needed. The models reported to estimate mass transfer coefficient are once again empirical in nature [11]. To reduce empiricism in mass transfer modeling, the mass transfer coefficient should be estimated from fundamental principles. Thus, using CFD models to understand interphase mass transfer for a single drop or a couple of drops and utilizing the resulting data to obtain CFD-based mass transfer coefficient models for use in equipment-level CFD models is necessary.

Of late, there has been significant research on microfluidic solvent extraction. Carrying out microfluidic solvent extraction leads to process intensification and can be used for variety of applications in the field of solvent extraction including extraction of radionuclides [12,13]. In microfluidic solvent extraction, two flowing immiscible liquid phases are brought into contact at a microfluidic junction. Depending on the flow rates of the phases, their physical properties and the design of microfluidic junction, different kinds of flow patterns may result. Slug flow, droplet flow, core-annular flow, parallel flow are some of the typical flow patterns which are obtained in microfluidic solvent extraction. The flow pattern which is likely to result when two immiscible flowing liquids are contacted at a microfluidic junction, the size of the dispersed phase (slug size, droplet size), their velocities in the microchannels and interphase mass transfer coefficients are the aspects relevant to microfluidic extraction which need to be understood [14,15]. CFD modeling can be carried out to investigate and understand these aspects of microfluidic solvent extraction.

In this article, we intend to give an overview of the studies which are being carried out at Chemical Engineering Division, BARC to use CFD modeling to understand the above-mentioned fundamental aspects relevant to solvent extraction.

CFD Modeling of Drag Phenomenon

To study the drag phenomenon in liquid-liquid systems, a single droplet surrounded by a flowing continuous phase is considered. A typical computational domain used for CFD modeling is shown in Fig. 1. It comprises a cube with a spherical drop placed at its centre. CFD simulation involves solution of Reynolds Averaged Navier-Stokes (RANS) equations in the continuous phase and Navier-Stokes equations in the drop phase. The key aspect of the modeling is capturing the effect of internal circulation inside the drop on the drag force exerted on it by the continuous phase and to capture the effect of continuous phase turbulence on drag coefficient. To capture the effect of internal circulation on drag coefficient, appropriate interfacial boundary conditions of velocity, shear stress and normal stress are required. Implementation of these interfacial boundary conditions helps capture the effect of internal circulation inside the droplet and its effect on drag force exerted by the continuous phase on the droplet. The governing equations and boundary conditions for flow simulations are described in our previous study [16].

The CFD model is validated by comparing the drag coefficient predicted by the CFD model with the drag coefficient estimated from the correlation analytical solution for creeping flow regime [17, 18]. For higher Reynolds number, validation is done by comparing drag coefficient predicted by the CFD model with drag coefficient estimated from the correlation reported by Harper and Moore [19]. The results of the validation summarized in Table 1 suggest a good agreement between the drag coefficient values predicted by the CFD model (C_{d_CFD}) and the same predicted by the analytical model (C_{d_anal}) and empirical correlation (C_{d_corr}). Fig. 2 shows the streamlines of internal circulation inside the drop and streamlines of the continuous phase outside the drop for two different particle Reynolds numbers. At higher particle Reynolds number, wake formation behind the drop is observed. The CFD model was further extended to estimate the effect of turbulence on drag coefficient. For this, simulations were

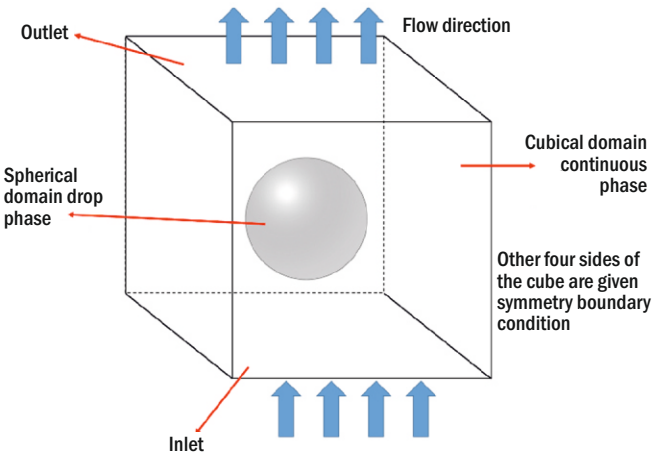

Fig.1: Typical computational domain used for CFD modeling of drag phenomenon.

carried out by introducing a source term in the equation of turbulent kinetic energy using the approach reported in literature to estimate the effect of turbulence on drag on a solid particle and a gas bubble for liquid-solid and gas-liquid systems [20,21]. The results from the CFD simulations were used to prescribe a CFD-based correlation to estimate the drag coefficient. The correlation, given by Eq. (1), has particle (drop) Reynolds number (Re_p), Kolmogorov length scale (λ), drop diameter (d) as the independent variables and predicts drag coefficient (C_d). Particle Reynolds number is defined by Eq. (2) in which ρ_c is the density of the continuous phase, μ_c is the viscosity of the continuous phase and $\vec{u}_{slip}$ is the slip velocity between the drop and the continuous phase.

$$C_d = \frac{(d/\lambda)^3 + 1.5031\, Re_p + 103.81}{0.0308 Re_p^2 - 2.0687 Re_p + 95.696} \quad (1)$$

$$Re_p = \frac{d\rho_c|\vec{u}_{slip}|}{\mu_c} \quad (2)$$

The drag coefficient correlation obtained from CFD simulations was implemented in equipment-level two-phase flow simulations of Pulsed Disc and Doughnut Column (PDDC) and a good prediction of dispersed phase holdup was obtained for different operating conditions. Thus, by replacing an empirical drag model with a CFD-based drag model, empiricism was reduced in the equipment-level CFD model. The CFD model to estimate drag coefficient is being further extended to estimate drag coefficient for concentrated liquid-liquid dispersions in which drag coefficient will depend, in addition to particle Reynolds number and Kolmogorov length scale, on dispersed phase holdup also.

Table1: Comparison of drag coefficient obtained from CFD model with drag coefficient estimated from analytical equation/empirical correlation.

Re_p	C_{d_corr} / C_{d_anal}	C_{d_CFD}	AARE (%)
	Creeping flow regime		
0.285	70.19	65.30	6.97
0.568	35.24	32.92	6.60
1.18	16.95	15.35	9.42
2.17	9.21	8.98	2.49
	High Reynolds number regime		
120.86	0.46	0.50	8.98
169.20	0.39	0.41	4.88
254.30	0.30	0.33	10.42
Average Absolute Relative Error (AARE)			7.11

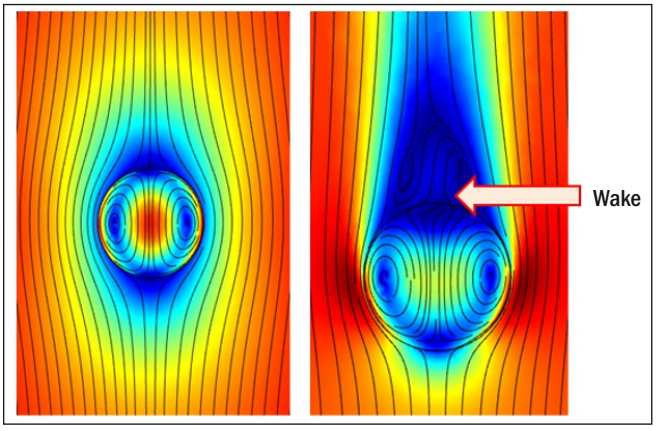

Fig.2: Streamlines inside and outside the drop at Re_p = 0.289 (left) and, Re_p = 254 (right).

CFD Modeling of Droplet Breakage and Coalescence

As discussed in the introduction section, breakage and coalescence is yet another important aspect which is fundamental to solvent extraction equipment. In a solvent extraction equipment, breakage of droplets can occur in different manners such as breakage due to turbulence and breakage due to shear. The breakage also significantly depends of the flow field. CFD modeling is being used to understand droplet breakage phenomena. To begin with, breakage of dispersed phase to form droplets under simpler settings has been studied. Some of the studies that have been done are studying droplet formation at top-submerged and bottom-submerged nozzles immersed in a quiescent continuous phase [22], drop formation on a single hole in a sieve plate and nozzle plate for quiescent continuous phase [23]. Drop formation under pulsatile flow of the dispersed phase at nozzles immersed in quiescent continuous phase has also been investigated [24]. Such CFD modeling typically involves interface-tracking simulations using methods such as Level Set or Volume of Fluid or Phase-field. The details of the computational models have been provided in our previous works [22,23]. Validation of CFD models has been done using in-house data [25,26] and data reported in literature [27]. Detailed insights are obtained from CFD simulations of drop breakage phenomena. For example, Fig. 3 shows the evolution of drop at a hole in a plate (a hole of a typical sieve plate) immersed in quiescent continuous phase for different velocities of the dispersed phase. The figure shows that the drop diameter and drop detachment height increase and drop detachment time reduces as the velocity of the dispersed phase through the sieve plate hole increases. Increase in drop detachment height with increase in dispersed phase velocity shows gradual transition toward jetting regime at higher velocities.

The studies have helped in understanding the effect of geometry (nozzle diameter, nozzle shape–flat versus sharp tip, diameter of plain hole and nozzle hole in a plate), physical properties (density difference, interfacial tension, contact angle) on diameter of drops produced as a result of breakage of the dispersed phase. Further studies on understanding phenomenon of drop breakage in different types of flow fields of the continuous phase such as counter-current flow, cross-current flow, rotational flow, and pulsatile flow, are going on. Extensive research is still needed to understand the droplet breakage in different types of turbulent flow fields typically observed in solvent extraction contactors.

While several studies have been done on drop breakage and formation, the computational studies on drop coalescence are scant. The coalescence, either interfacial or binary, involves drainage of the film between drop and its bulk phase or between two drops. Resolving of the film during drainage requires very fine mesh and very small time step size which makes CFD modeling of drop-level coalescence phenomenon computationally very challenging. Very few studies on CFD modeling of coalescence phenomenon have been reported [28]. Most of them are for coalescence of a drop with its bulk phase (interfacial coalescence). Studies on binary coalescence are rare. Extensive work is needed to understand various aspects of coalescence phenomenon such as binary coalescence, effect of interface-seeking impurities on coalescence, coalescence in pulsatile flow as is observed in the disengagement sections of pulsed columns etc.

CFD Modeling to Estimate Mass Transfer Coefficient

The CFD model described above for studying drag phenomenon can be extend to study mass transfer

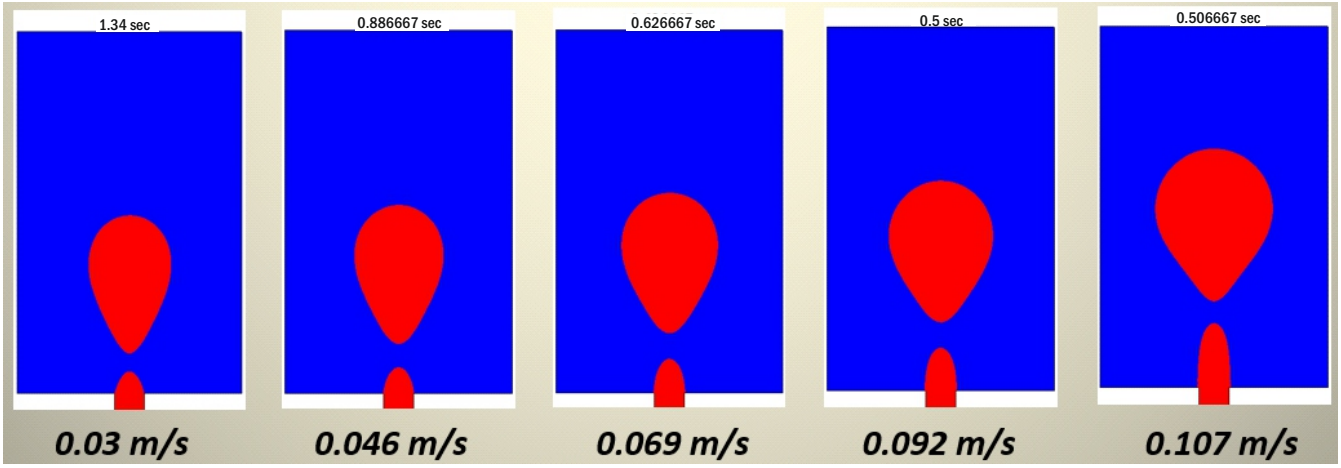

Fig.3: CFD modeling of drop formation at a hole in a plate immersed in a quiescent continuous phase for different velocities of the dispersed phase.

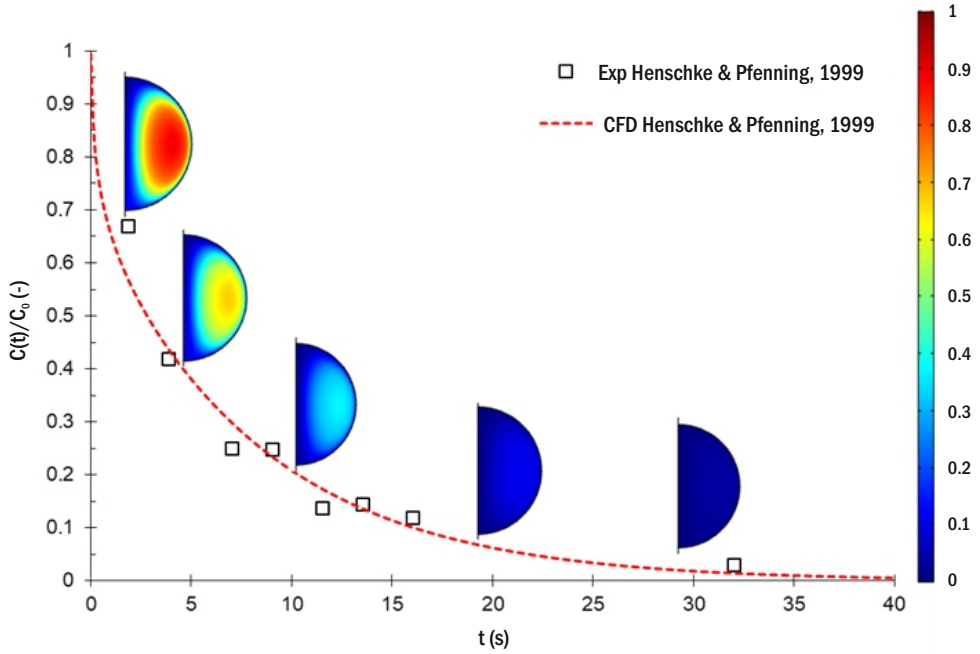

Fig.4: Comparison of CFD-predicted and reported variations of the normalized average concentration of the solute in a drop with time.

phenomenon also. For this, species transport equation needs to be solved additionally in the continuous phase and the drop phase after applying appropriate boundary conditions (concentration jump and continuity of mass transfer flux) at the liquid-liquid interface. The detailed description of the CFD modeling for estimation of mass transfer coefficient is provided in our previous study [16]. The model predicts the change in concentration of a solute inside the drop with time due to its mass transfer to the continuous phase flowing past the drop. The concentration–time profile can be further processed to estimate mass transfer coefficient and hence Sherwood number. The model has been validated by comparing the concentration-time profile obtained from the model with the same reported in the literature [29], as shown in Fig. 4 which also shows the dimensionless solute concentration profiles in one half of the drop at different instants of time. It may be noted that concentration of the solute in the drop gradually reduces with time. As there is a circulation inside the drop, mass transfer near the interface and center of the drop is convection controlled but at the center of the circulation inside the drop, mass transfer is mainly diffusion controlled as the convective transport is minimum there. Hence, the slowest variation of concentration inside the droplet is observed in the vicinity of the center of the circulation inside the drop.

The model has been used to study the effect of shape of droplets on mass transfer. For this, comparison was done between spherical droplets, symmetrical ellipsoidal droplets and asymmetrical ellipsoidal droplets. Such simulations reveal some interesting results. For example, in some cases, ellipsoidal drops are found to have two internal circulation vortices in one half of the drop. Presence of secondary circulation vortex is found to enhance the mass transfer rate. The CFD model for estimating mass transfer was further used for studying mass transfer in pulsatile flow of the continuous phase. Pulsatile flow is important for air pulsed columns. The results of the simulations show that pulsatile flow of continuous phase leads to significant enhancement of mass transfer compared to the case of steady flow of the continuous phase. The results from CFD simulations were used to obtain a correlation to estimate Sherwood number (*Sh*) with particle

Reynolds number (Re_p), Schmidt number (Sc) as the independent variables for mass transfer from a spherical droplet. The correlation is given by Eq. (3). The values of the physical properties used to estimate particle Reynolds number and Schmidt number are the geometrical means of the physical properties of the two phases. The same correlation is found to be suitable for pulsatile flow of the continuous phase if pulsing velocity is also taken into account for calculating particle Reynolds number. The CFD-based correlation for estimating Sherwood number was implemented in axial dispersion model to simulate extraction of uranium in a pulsed disc and doughnut column. The predicted concentration profiles and end concentrations were found to be more accurate when CFD based correlation for Sherwood number was used compared to the case when an empirical model for estimating Sherwood number was used.

$$Sh = 2 + 0.00085{Re_p}^{1.13}Sc^{0.98} \quad (3)$$

CFD Modeling for Microfluidic Solvent Extraction

As mentioned earlier, there is lot of research going on in the field of microfluidic extraction, which is basically a process intensification tool. Several studies have been reported on microfluidic extraction of nuclear materials [30-34]. While majority of these studies have been experimental in nature, numerical simulations find applications in understanding various aspects relevant to solvent extraction in microchannel. In a typical microfluidic extraction system, a flowing aqueous phase is contacted with a flowing organic phase at a microfluidic junction. When the two phases come in contact at the microfluidic junction, depending on the geometry and material of construction of the junction, one of the phases may get dispersed in the continuum of the other. Depending on the flow rates, design of the microfluidic junction (T-junction, Y-junction etc.), physical properties of the two liquid phases (viscosity and interfacial tension) different types of flow patterns may emerge. Some typical flow patterns are slug flow, droplet flow, finely dispersed flow, slug and droplet flow, core-annular flow and parallel flow. Slug flow, droplet flow and finely dispersed flow are dispersed flow patterns in which dispersed phase breaks down in discrete entities. Parallel and core-annular flow are non-dispersive flow patterns in which two phases do not mix but flow along the microchannel with a continuous liquid-liquid interface. CFD modeling can be used to understand different aspects of microfluidic extraction. It can be used to find out the kind of flow pattern and size of the dispersed phase entities that will be generated at a microfluidic junction for a given liquid-liquid system, geometry of the microfluidic junction and flow rates of the liquids. It can also be used to estimate the velocity of the slugs/drops flowing in the microchannel and to estimate the interphase mass transfer coefficients. Prediction of the flow pattern, size of the dispersed phase (drop diameter/slug length) and mass transfer coefficients can help predict the mass transfer expected in a microfluidic extraction system.

To predict the flow pattern expected at a microfluidic junction, interphase capturing/tracking simulations are required. This typically involves solving the continuity and momentum equations while using an interface-capturing/tracking method such as Volume of Fluid (VOF)/level-set/phase-field/Arbitrary Lagrangian-Eulerian framework [35]. Further, to quantify interphase mass transfer inside the microchannel, simulations can be done for the fixed liquid-liquid interface if it is known priori. The dispersed entities (slug/drops) are periodic in nature. Thus, single unit cell approach can be used in which a periodic domain comprising a single drop or slug and continuous phase surrounding it can be used after applying proper boundary conditions at the periodic boundaries, at the interface between the two-phases and the other boundaries defining the computational domain [36,37]. Simulations typically involve solving Navier-Stokes equations for the two phases (continuous phase, slug/drop phase) followed by solution of species transport equations in the two phases with one way coupling between hydrodynamics and mass transfer. Applications of appropriate boundary conditions at the liquid-liquid interface helps in capturing internal circulation inside the drop/slug. The velocity of the slug/drop can be found out by finding the mixture velocity for which the drag force exerted on the slug/drop becomes zero as in a microchannel the drops/slugs eventually move at a constant speed [36]. With slug/drop size, slug/drop velocity and interphase mass transfer coefficients known, it is possible to estimate the mass transfer expected from a given microfluidic extraction system [38].

Simulations to predict the liquid-liquid flow pattern expected at a microfluidic junction have been carried out and validated with reported data [35]. Simulations of slug flow and droplet flow in microchannels have also been carried out and validated with in-house and reported experimental data. Fig. 5(a) and Fig. 5(b) show typical flow field obtained from CFD simulations of droplet flow and slug flow, respectively, in a circular microchannel. Internal circulations inside the slug/drop can be observed clearly.

Simulations in case of non-dispersive microfluidic liquid-liquid flows such as core-annular flow (CAF) or parallel flow (PF) are easier, as tracking of liquid-liquid interface is not required in such flows. The position of the interface can be obtained analytically [39]. CFD modeling of such non-dispersive flows has been carried out to fundamentally understand the phenomenon of liquid-liquid mass transfer in such flows [39]. Fig. 5(c) shows typical velocity field obtained from CFD simulations of core-annular flow in microchannel. CFD model of flow and mass transfer in CAF was used to perform parametric analysis and the resultant data were used for obtaining correlations to estimate Sherwood numbers for the core (Sh_c) and annulus (Sh_a) for liquid-liquid mass transfer in CAF. The correlations are given by Eqs. (4) and (5) where z is

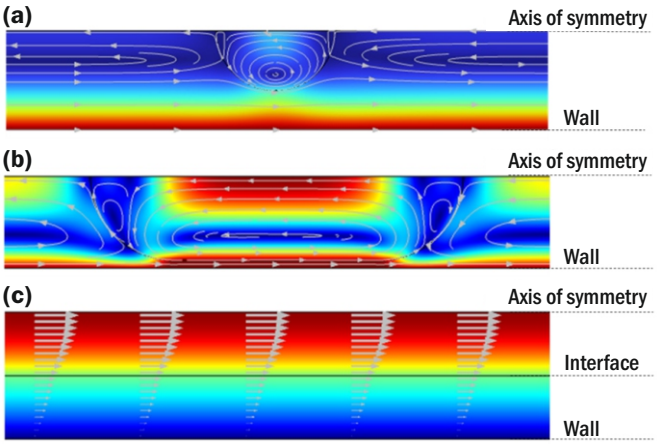

Fig.5: Typical velocity profiles and streamlines/ velocity vectors in (a) droplet flow and (b) slug flow (c) core-annular flow as obtained from CFD simulations carried out to study flow field and mass transfer in microchannels ((a) and (b): velocity field in droplet frame of reference using unit cell approach; c: velocity field in lab frame of reference; blue and red colors represent zero and maximum velocity magnitude respectively in rainbow color scale; geometries are axisymmetric).

axial position, D_{hc} and D_{ha} are hydraulic diameter for the core and annulus respectively, Re_c and Re_a are the Reynolds numbers for core and annulus respectively and Sc_c *and* Sc_a are the Schmidt numbers for the core and the annulus respectively.

$$Sh_c = 1.0901\, Re_c^{0.5053} \left(\frac{z}{D_{hc}}\right)^{-0.5053} Sc_c^{0.5053} \quad (4)$$

$$Sh_a = 0.4401\, Re_a^{0.4512} \left(\frac{z}{D_{ha}}\right)^{-0.4512} Sc_a^{0.4512} \quad (5)$$

Similar correlations are being obtained to estimate Sherwood number in droplet and slug flow regimes based on the regression of data resulting from parametric analysis done using validated CFD models for simulating hydrodynamics and mass transfer in droplet and slug flow regimes.

Conclusions

The present article provides an overview of how CFD can be used as an effective tool to simulate and understand the fundamental phenomena relevant to solvent extraction. Such CFD studies typically involve simulations at the level of a single droplet. The results from such simulations can be used to obtain the CFD-based laws/correlation/equations to replace the empirical correlations which are typically used as closure equations in equipment-level CFD simulations of solvent extraction equipment. Thus, apart from understanding fundamental phenomena relevant to solvent extraction, CFD modeling of fundamental phenomena relevant to solvent extraction eventually helps in reducing empiricism in equipment-level CFD models. CFD simulations of such phenomena are also very useful as conducting experimental studies at a single drop level is usually difficult.

CFD simulations have been carried out to understand the phenomenon of drag in liquid-liquid system in which the effect of internal circulation inside the droplet and turbulence in the continuous phase on drag coefficient has been captured. A CFD-based drag model has been obtained and implemented in equipment-level CFD model. Similarly, CFD studies have been performed to understand the phenomena of drop formation at nozzles and holes in plates submerged in quiescent continuous phase. However, further studies are required to understand the drop formation and droplet breakage in complex flow conditions of the continuous phase. Mass transfer from a single droplet has been studied in detail by developing a CFD model which captures the effect of internal circulation inside the droplet on mass transfer. A CFD-based correlation has been obtained to estimate Sherwood number for mass transfer from a spherical droplet under steady and pulsatile flow of the continuous phase. This CFD-based correlation has been implemented in equipment-level mass transfer models and is found to work well. Effect of shape of the droplet on mass transfer has also been studied using CFD. However, further studies are needed to understand mass transfer in presence of Marangoni convection and mass transfer from deformable droplets.

Extensive work has been carried out to understand liquid-liquid two-phase flow and mass transfer in microchannels which are being explored for intensification of solvent extraction processes. CFD simulations have been carried out to fundamentally understand liquid-liquid two-phase flow hydrodynamics and mass transfer in different flow regimes (slug flow, droplet flow, core-annular flow) in microchannels. Further understanding is required to quantify the extent of mass transfer during formation of slugs and droplets at microfluidic junctions through computationally more challenging models. The quantitative data resulting from such CFD simulations can help design efficient microfluidic systems for different separation tasks.

References

[1] H. Singh, and C.K. Gupta, Mineral Processing and Extractive Metallurgy Review, 2000, 21 (1-5), 307.

[2] R. Natarajan, Progress in Nuclear Energy, 2017, 101, 118.

[3] R. Yadav, and A.W. Patwardhan, Chemical Engineering Journal, 2008, 138(1-3), 389.

[4] K.K. Singh, S. Sarkar, N. Sen, S. Mukhopadhyay, and K.T. Shenoy, BARC Newsletter, 2021, Nov.-Dec., 45.

[5] N. Sen, K.K. Singh, A.W. Patwardhan, S. Mukhopadhyay, and K.T. Shenoy, Separation Science & Technology, 2016, 51(17), 2790.

[6] S. Sarkar, K.K. Singh, S.M. Mahajani, and K.T. Shenoy, Solvent Extraction and Ion Exchange, 2020, 38(5), 536.

[7] K.K. Singh, S.M. Mahajani, K.T. Shenoy, and S.K. Ghosh, Industrial Engineering Chemistry Research, 2009,48(17): 8121-8133.

[8] N. Sen, K.K. Singh, A.W. Patwardhan, S. Mukhopadhyay, and K.T. Shenoy, CFD modelling to predict mass transfer in pulsed sieve plate extraction columns.12th International Conference on Computational Fluid Dynamics in the Oil & Gas, Metallurgical and Process Industries (CFD-2017), 30 May- 1 June (2017), Trondheim, Norway.

[9] J.-Q. Liu, S.-W. Li, Y.-Y. Wang, Q. Zhang, and S. Jing, Solvent Extraction and Ion Exchange, 2017, 3, 187-198.

[10] S. Sarkar, K.K. Singh, and K.T. Shenoy, BARC Newsletter, 2017, 360, 18.

[11] K. Gonda, and T. Matsuda, Journal of Nuclear Science and Technology, 1986, 23(10), 883.

[12] N. Sen, M. Darekar, P. Sirsat, K.K. Singh, S. Mukhopadhyay, S.R. Shirsath, and K.T. Shenoy, Separation and Purification Technology, 2019, 227, 1156641.

[13] D. Tsaoulidis, V. Dore, P. Angeli, N.V. Plechkova, and K.R. Seddon, Chemical Engineering Journal, 2013, 227, 151.

[14] M.N. Kashid, D.W. Agar, and S. Turek, Chemical Engineering Science, 62(18-20), 5102.

[15] J. Yin, and S. Kuhn, Chemical Engineering and Processing: Process Intensifications, 2023, 190, 109414.

[16] S. Sarkar, K.K. Singh, and K.T. Shenoy, Chemical Engineering Science, 2023, 267, 118240.

[17] J.S. Hadamard, Seances Acad. Sci. Paris, 1911,152, 1735.

[18] W. Rybczynski, Bull. Acad. Sci. Cracovie A, 1911, 1, 40.

[19] J.F. Harper, and D.W. Moore, Journal of Fluid Mechanics, 1968, 32(2), 367-391.

[20] A.R. Khopkar, and V.V. Ranade, AIChE Journal, 2006, 52(5), 1654.

[21] A.R. Khopkar, G.R. Kasat, A.B. Pandit, and V.V. Ranade, Industrial and Engineering Chemistry Research, 2006, 45(12), 4416.

[22] A. Roy, N. Sen, K.K. Singh, K.T. Shenoy, and R.B. Grover, Solvent Extraction & Ion Exchange, 2019, 37(2), 191.

[23] N. Sen, K.K. Singh, S. Mukhopadhyay, and K.T. Shenoy, Chemical Engineering Communications,2019, 206(10), 1317.

[24] S. Agarwal, N. Sen, G. Sugilal, and K.K. Singh, Comparison of drop formation at sieve plate hole under pulsatile and non-pulsatile flow: a CFD study, 15th Biennial DAE-BRNS Symposium on Nuclear and

Radiochemistry (NUCAR-2021), 22-26 February (2022), DAE Convention Centre, Anushaktinagar, Mumbai, India.

[25] A. Roy, M. Darekar, K.K. Singh, and K.T. Shenoy, Nuclear Engineering & Technology, 2019, 51(3), 761.

[26] A. Roy, M. Darekar, K.K. Singh, K.T. Shenoy, and R.B. Grover, Nuclear Science & Techniques, 2018, 29(6), 88.

[27] A. Soleymani, A. Laari, and I. Turunen, Chemical Engineering Research and Design, 2008, 86(7), 731.

[28] F. Gebauer, M. W. Hlawitschka, and H.-J. Bart, Chinese Journal of Chemical Engineering, 2016, 24(2), 249.

[29] M. Henschke, and A. Pfennig, AIChE Journal, 1999,45(10), 2079.

[30] N. Sen, K.K. Singh, S. Mukhopadhyay, and K.T. Shenoy, Chemical Engineering Research and Design, 2022, 177, 83.

[31] C. Mariet, A. Vansteene, M. Losno, J. Pellé, J.P. Jasmin, A. Bruchet, and G. Hellé, Micro and Nano Engineering, 2019, 3, 7.

[32] A. Abbasi, A. Rahbar-Kelishami, and M.J. Ghasemi, Journal of Rare Earths, 2018, 36(11), 1198.

[33] M. Darekar, K.K. Singh, P. Sapkale, A.K. Goswami, S. Mukhopadhyay, and K.T. Shenoy, Chemical Engineering and Processing-Process Intensification, 2018, 132, 65.

[34] D. Tsaoulidis, and P. Angeli, Chemical Engineering Journal, 2015, 262, 785-793.

[35] K.K. Singh, K.T. Shenoy, H. Rao, and S.K. Ghosh, Numerical simulation of liquid-liquid two-phase flow at microfluidic junctions, 3rd European Conference on Microfluidics (μFlu'12), 3-5 December (2012), Heidelberg, Germany.

[36] D. Mikaelian, B. Haut, and B. Scheid, Microfluidics and Nanofluidics, 2015, 19, 523.

[37] J. Rivero-Rodriguez, and B. Scheid, Journal of Fluid Mechanics, 2019, 869, 110.

[38] R.K. Chaurasiya, K.K. Singh, S. Chakraborty, S. Mukhopadhyay, and S. Sarkar. Conceptual design of process for solvent extraction of uranium using core-annular flow in microchannels, International Solvent Extraction Conference (ISEC-2022), 26-30 September (2022), Gothenburg, Sweden.

[39] R.K. Chaurasiya, and K.K. Singh, Chemical Engineering Science, 2022, 249, 117295.